

M.A. Silaev^{1,2} and G.E. Volovik^{2,3*}

Topological superfluid $^3\text{He-B}$: fermion zero modes on interfaces and in the vortex core

October 22, 2018

Keywords topological superfluid, $^3\text{He-B}$, relativistic superconductor, index theorem

Abstract Many quantum condensed matter systems are strongly correlated and strongly interacting fermionic systems, which cannot be treated perturbatively. However, topology allows us to determine generic features of their fermionic spectrum, which are robust to perturbation and interaction. We discuss the nodeless 3D system, such as superfluid $^3\text{He-B}$, vacuum of Dirac fermions, and relativistic singlet and triplet superconductors which may arise in quark matter. The systems, which have nonzero value of topological invariant, have gapless fermions on the boundary and in the core of quantized vortices. We discuss the index theorem which relates fermion zero modes on vortices with the topological invariants in combined momentum and coordinate space.

PACS numbers: 67.30.H- , 11.27.+d , 73.20.-r , 72.80.Sk

1 Introduction

Fully gapped 3-dimensional fermionic systems – topological insulator and topological superconductors – are now under extensive investigation. The interest to such systems is revived after identification of topological insulators in compounds $\text{Bi}_{1-x}\text{Sb}_x$, Bi_2Te_3 , Bi_2Se_3 (see review¹). These systems are characterized by the gapless fermionic states on the boundary of the bulk insulator or at the interface between different states of the insulator. Historically, the topological insulators have been introduced in Ref.², and the first example of fermion zero modes at the interface was provided in Ref.³. At the moment the term ‘strong topological

1: Institute for Physics of Microstructures RAS, 603950 Nizhny Novgorod, Russia
E-mail: msilaev@mail.ru

2: Low Temperature Laboratory, Aalto University, P.O. Box 15100, FI-00076 AALTO, Finland

3: L.D. Landau Institute for Theoretical Physics, 119334 Moscow, Russia

* Tel.: +358-9-4512963, Fax: +358-9-4512969, E-mail: volovik@boojum.hut.fi

insulator' refers to time reversal invariant insulators with odd number of Dirac points within the Fermi surface on the surface of insulator, such as Bi_2Te_3 ^{1,4}. The example of the fully gapped topological superfluids is superfluid $^3\text{He-B}$, discovered in 1972⁵. The topological invariant for $^3\text{He-B}$ and the gapless states at the interface between bulk states with different topological charges were discussed in Ref.⁶. The modern theoretical treatment of topological insulators and superfluids/superconductors in three spatial dimensions can be found in^{7,8,9,10}.

Fully gapped 3-dimensional fermionic systems may arise also in relativistic quantum field theories. In particular, the Dirac vacuum of massive Standard Model particles has also the nontrivial topology, and the domain wall separating vacua with opposite signs of the mass parameter M contains fermion zero modes¹¹. Topologically nontrivial states may arise in dense quark matter, where chiral and color superconductivity is possible. The topological properties of such fermionic systems have been recently discussed in Ref.¹². In particular, in some range of parameters the isotropic triplet relativistic superconductor is topological and has the fermion zero modes both at the boundary and in the vortex core. On the other hand, there is a range of parameters, where this triplet superconductor is reduced to the non-relativistic superfluid $^3\text{He-B}$ ¹³. That is why the analysis in Ref.¹² is applicable to $^3\text{He-B}$ and becomes particularly useful when the fermions living in the vortex core are discussed.

In relativistic theories there is an index theorem which relates the number of fermion zero modes localized on a vortex with the vortex winding number¹⁵. However, the analysis in Ref.¹² suggests, that this theorem is valid only for vortices in topological vacua (the Dirac vacuum considered in Ref.¹⁵ is topological, see¹⁶). It is possible that there exists a more general index theorem which relates the number of fermion zero modes localized on a vortex not only to the vortex winding number, but also to the topological charge of the bulk vacuum or superconductor.

Here we consider the phase diagrams of the topologically different states of isotropic triplet superconductors in relativistic regime and in the non-relativistic weak coupling and strong coupling regimes, and the fermion zero modes on domain walls and vortices in these regimes. It appears that in all systems, which we considered, a nonzero value of topological invariant in the bulk system automatically leads to existence of gapless fermions in the core of quantized vortices. We also demonstrate an example of the index theorem, which expresses the number of fermion zero modes on a vortex through the topological invariant in the combined coordinate and momentum space.

2 Superfluid relativistic medium and $^3\text{He-B}$

In relativistic superconductor or superfluid with the isotropic pairing – such as color superconductor in quark matter – the fermionic spectrum is determined by Hamiltonian

$$H = \tau_3 (c\alpha \cdot \mathbf{p} + \beta M - \mu_R) + \tau_1 \Delta, \quad (1)$$

for spin singlet pairing, and by Hamiltonian

$$H = \tau_3 (c\alpha \cdot \mathbf{p} + \beta M - \mu_R) + \gamma_5 \tau_1 \Delta, \quad (2)$$

for spin triplet pairing^{13,12}. Here α^i , β and γ_5 are Dirac matrices, which in standard representation are

$$\alpha = \begin{pmatrix} 0 & \sigma \\ \sigma & 0 \end{pmatrix}, \quad \beta = \begin{pmatrix} 1 & 0 \\ 0 & -1 \end{pmatrix}, \quad \gamma_5 = \begin{pmatrix} 0 & 1 \\ 1 & 0 \end{pmatrix}; \quad (3)$$

M is the rest energy of fermions; μ_R is their relativistic chemical potential as distinct from the non-relativistic chemical potential μ ; τ_a are matrices in Bogoliubov-Nambu space; and Δ is the gap parameter.

In non-relativistic limit the low-energy Hamiltonian is obtained by standard procedure, see e.g.¹⁷. The non-relativistic limit is determined by the conditions

$$cp \ll M \quad (4)$$

and

$$|M - \sqrt{\mu_R^2 + \Delta^2}| \ll M. \quad (5)$$

Under these conditions the Hamiltonian (1) reduces to the Bogoliubov - de Gennes (BdG) Hamiltonian for fermions in spin-singlet s -wave superconductors, while (2) transforms to the BdG Hamiltonian relevant for fermions in isotropic spin-triplet p -wave superfluid ³He-B:

$$H = \tau_3 \left(\frac{p^2}{2m} - \mu \right) + c^B \tau_1 \sigma \cdot \mathbf{p}, \quad m = \frac{M}{c^2}, \quad c^B = c \frac{\Delta}{M}, \quad (6)$$

where the nonrelativistic chemical potential $\mu = \sqrt{\mu_R^2 + \Delta^2} - M$. According to the Eq.(5) the non-relativistic Hamiltonian is relevant only if $|\mu| \ll M$. The Fermi liquid corrections are missing in this approach, which in particular must give the effective mass m^* instead of the bare mass m of ³He atom. But this is not important for topological consideration.

Note that we do not put any additional constraint on the value of the gap Δ , which in principle can be comparable with the rest energy M , and as a result the velocity of particles $\partial\varepsilon/\partial p$ may approach the speed of light c even in the non-relativistic limit $cp \ll M$. The special discussion is needed for the case when $\Delta > M$. In this case one has $c_B > c$, and Eq.(6) suggests that particles may propagate with velocity $|\partial\varepsilon/\partial p| > c$, which certainly is not correct since particles cannot move faster than light. In this case of the large gap one should take into account the relativistic corrections to the coefficient c^B in Eq.(6):

$$c^B \approx \frac{\Delta}{M} \left(1 - \frac{\mu}{2M} - \frac{c^2 p^2}{4M^2} + \dots \right). \quad (7)$$

These corrections together with conditions (4) and (5) provide the validity of equation $|\partial\varepsilon/\partial p| < c$ for the whole range of parameters.

The Dirac-BdG system in Eq.(2) has the following spectrum

$$\varepsilon = \pm \sqrt{M^2 + c^2 p^2 + \Delta^2 + \mu_R^2} \pm 2 \sqrt{M^2 (\mu_R^2 + \Delta^2) + \mu_R^2 c^2 p^2}. \quad (8)$$

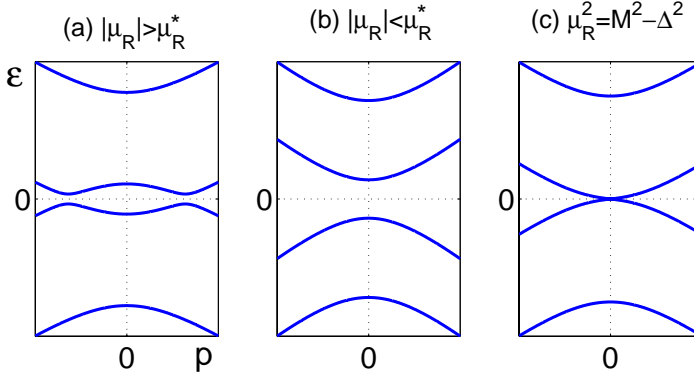


Fig. 1 Plot of the spectrum of relativistic Hamiltonian (2) for two generic cases: (a) $|\mu_R| > \mu_R^*$ and (b) $|\mu_R| < \mu_R^*$. The gap in the spectrum closes at $\mu_R^2 = M^2 - \Delta^2$ which is shown in plot (c).

This spectrum is plotted in Fig.1. Depending on the value of the parameters μ_R , Δ , M the spectral branches have different configurations.

There is a soft quantum phase transition, at which the position of the minimum of energy $E(p)$ shifts from the origin $\mathbf{p} = 0$, and the energy profile forms the Mexican hat in momentum space. This momentum-space analog of the Higgs transition¹⁴ occurs when the relativistic chemical potential μ_R exceeds the critical value

$$\mu_R^* = \left(\frac{M^2}{2} + \sqrt{\frac{M^4}{4} + M^2 \Delta^2} \right)^{1/2}. \quad (9)$$

Fig.1 demonstrates two generic cases: $|\mu_R| > \mu_R^*$ when there are extremums of function $\varepsilon(p)$ at $p \neq 0$ and $|\mu_R| < \mu_R^*$ when all extremums are at the point $p = 0$.

The spectrum of non-relativistic BdG Hamiltonian is plotted in Fig.2. In the non-relativistic limit the soft quantum transition takes place at $\mu^* = mc_B^2 = \Delta^2/M$. But condition for derivation of the non-relativistic limit Eq.(5) yields $|\mu| \ll M$. This condition implies that the critical value μ^* is in the range of applicability of non-relativistic limit only when $|\Delta| \ll M$. For large Δ the Mexican hat is formed outside the non-relativistic range.

The formation of the Mexican hat at $|\mu_R| > \mu_R^*$ is an example of non-topological quantum phase transition. Now we turn to the topological quantum phase transitions, at which the topological invariant changes.

3 Topology of relativistic medium and $^3\text{He-B}$

There is a characteristic line $\mu_R^2 + \Delta^2 = M^2$ at which the gap in the spectrum closes (see Fig.1c). In non-relativistic limit the node in the spectrum takes place at $\mu = 0$ (see Fig.2c). This line corresponds to the topological quantum phase transition. The vacuum states with $\mu_R^2 + \Delta^2 > M^2$ and $\mu_R^2 + \Delta^2 < M^2$ are characterized by different values of the topological invariant, and thus cannot be adiabatically

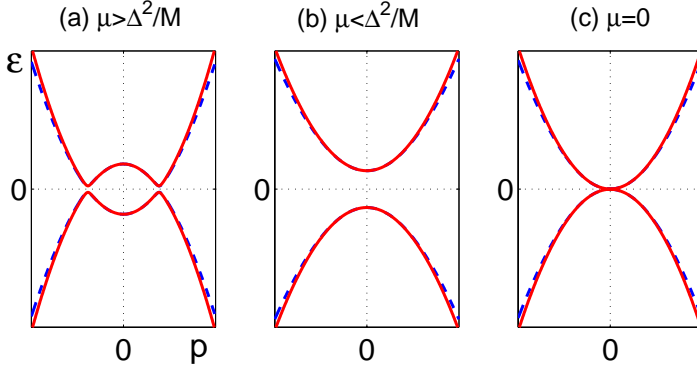


Fig. 2 Non-relativistic spectrum of Hamiltonian (6) (red solid lines) compared with the exact spectrum of relativistic Hamiltonian (2) plotted by blue dash lines (only the lowest energy branches are shown). The two generic cases correspond to: (a) $\mu > \Delta^2/M$ and (b) $\mu < \Delta^2/M$. The gap in the spectrum closes at $\mu = 0$ which is shown in plot (c).

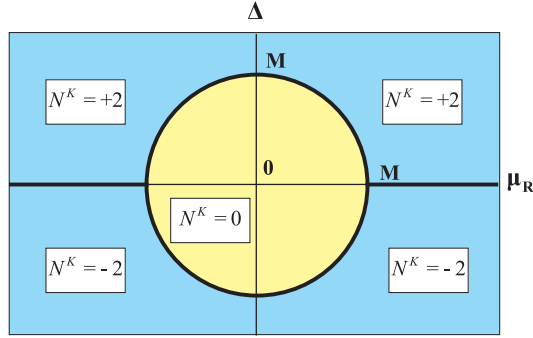


Fig. 3 Phase diagram of ground states of relativistic triplet superfluid in Eq.(2) in the plane (μ_R, Δ) . Topological quantum phase transitions are marked by thick lines. The states inside the circle $\mu_R^2 + \Delta^2 = M^2$ are topologically trivial. The states outside this circle represent topological superconductors. The states on the lines of topological quantum phase transition are gapless.

connected. Discontinuity in the topological charge across the transition induces discontinuity in energy across the transition. For example, for the 2+1 $p_x + p_y$ superfluid/superconductor the phase transition is of third order, meaning that the third-order derivative of the ground state energy is discontinuous²⁰.

The topological invariants which describe the fully gapped superconductors/superfluids, relativistic or non-relativistic, have the following form^{19,16}

$$N^K = \frac{e_{ijk}}{24\pi^2} \mathbf{tr} \left[\int d^3p K H^{-1} \partial_{p_i} H H^{-1} \partial_{p_j} H H^{-1} \partial_{p_k} H \right], \quad (10)$$

where the matrix K reflects the symmetry of the system: it commutes or anti-commutes with the Hamiltonian. The same invariants are applicable to the interacting systems, but instead of Hamiltonian, the Green's function matrix at zero

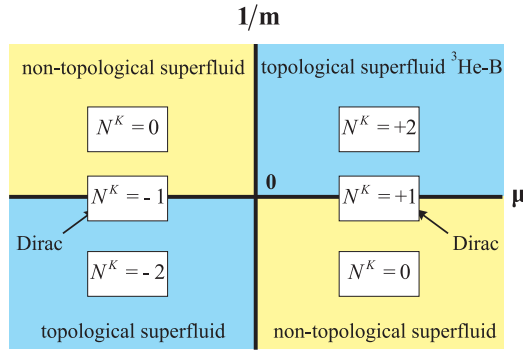


Fig. 4 Phase diagram of topological states of ${}^3\text{He-B}$ in Eq.(6) in the plane $(\mu, 1/m)$. States on the line $1/m = 0$ correspond to the Dirac vacua, which Hamiltonian is non-compact. Topological charge of the Dirac fermions is intermediate between charges of compact ${}^3\text{He-B}$ states. The line $1/m = 0$ separates the states with different asymptotic behavior of the Green's function at infinity: $G^{-1}(\omega = 0, \mathbf{p}) \rightarrow \pm \tau_3 p^2 / 2m$. The line $\mu = 0$ marks topological quantum phase transition, which occurs between the weak coupling ${}^3\text{He-B}$ (with $\mu > 0$, $m > 0$ and topological charge $N^K = 2$) and the strong coupling ${}^3\text{He-B}$ (with $\mu < 0$, $m > 0$ and $N^K = 0$). This transition is topologically equivalent to quantum phase transition between Dirac vacua with opposite mass parameter $M = \pm|\mu|$, which occurs when μ crosses zero along the line $1/m = 0$. The interface which separates two states contains single Majorana fermion in case of ${}^3\text{He-B}$, and single chiral fermion in case of relativistic quantum fields. Difference in the nature of the fermions is that in Bogoliubov-de Gennes system the components of spinor are related by complex conjugation. This reduces the number of degrees of freedom compared to Dirac case.

frequency must be used, $H(\mathbf{p}) \rightarrow G^{-1}(\omega = 0, \mathbf{p})$ ^{19,16}. The Green's function is the right object for the topological classification of vacuum states, because it automatically takes into account interaction and works even in cases when the effective single-particle Hamiltonian is not available. In simple cases when the single-particle Hamiltonian can be introduced the invariants can be transformed to the forms proposed in the modern literature. For application of the Green's function for topological classification of gapless and fully gapped systems, see the book²¹ and review²².

For ${}^3\text{He-B}$ in Eq.(6) and for triplet relativistic superconductor in Eq. (2) the relevant matrix $K = \tau_2$. This matrix K , which anti-commutes with the Hamiltonian, is the combination of time reversal and particle-hole symmetries. Fig. 3 shows the phase diagram of the vacuum states of relativistic triplet superconductors. The states inside the circle $\mu_R^2 + \Delta^2 = M^2$ are topologically trivial, while the states outside this circle represent topological superconductivity¹². The states on the lines of topological quantum phase transition are gapless.

Fig. 4 shows the phase diagram of the ground states of non-relativistic ${}^3\text{He-B}$ in the plane $(\mu, 1/m)$. The negative mass m may appear in the band structure in crystals. The topological quantum phase transition occurs at the critical value $\mu = 0$, which corresponds to the relativistic criterion $\mu_R = \sqrt{M^2 - \Delta^2}$. On the line $1/m = 0$ the Hamiltonian simulates that of free Dirac fermions with the mass parameter $M = \mu$ and the effective speed of light $c_{\text{eff}} = c_B$. The vacuum of free

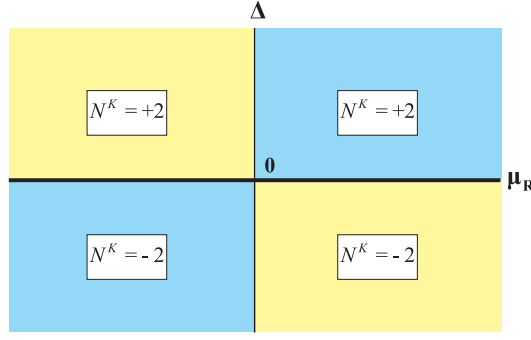


Fig. 5 Phase diagram of topological states of relativistic singlet superfluid with $M = 0$ in Eq.(1) in the plane (μ_R, Δ) .

Dirac vacuum fermions has topological charge

$$N^K = \text{sign}(M). \quad (11)$$

The real superfluid ${}^3\text{He-B}$ lives in the weak-coupling corner of the phase diagram: $\mu > 0, m > 0, mc^2 \gg \mu \gg mc_B^2$. However, in the ultracold Fermi gases with triplet pairing the strong coupling limit with $\mu < mc_B^2$ is possible near the Feshbach resonance²³. When μ crosses the value $\mu^c = 0$, the topological quantum phase transition occurs, at which the topological charge N^K changes from $N^K = 2$ to $N^K = 0$.

The singlet relativistic superconductor may also have the nontrivial topology. This happens if superconductivity occurs in the system of massless fermions of Standard Model. The equation (1) with $M = 0$, has additional symmetry. This symmetry leads to the matrix $K = \gamma_5 \tau_2$, which anti-commutes with Hamiltonian (1) at $M = 0$. The phase diagram of states of the relativistic singlet superconductor at $M = 0$ is shown in Fig. 5.

4 Gapless boundary states

The simplified Hamiltonians describing the boundary states on the surface of topological superfluids or at the interface between the bulk states:

$$\hat{H} = \tau_3 (c\alpha \cdot \hat{\mathbf{p}} + \beta M - \mu_R) + \gamma_5 \tau_1 \Delta(z), \quad (12)$$

$$\hat{H} = \tau_3 (c\alpha \cdot \hat{\mathbf{p}} - \mu_R) + \tau_1 \Delta(z), \quad (13)$$

$$\hat{H} = \tau_3 \left(\frac{\hat{\mathbf{p}}^2}{2m} - \mu \right) + \tau_1 \left(c_x^B(z) \hat{p}_x \sigma_x + c_y^B(z) \hat{p}_y \sigma_y + \frac{1}{2} \{c_z^B(z), \hat{p}_z\} \sigma_z \right), \quad (14)$$

$$\hat{H} = c \tau_3 \sigma \cdot \hat{\mathbf{p}} + M(z) \tau_1. \quad (15)$$

Equations (12) and (13) describe the boundary/interfaces of triplet and singlet relativistic superconductors correspondingly. The singlet relativistic superconductor is formed by massless relativistic fermions, $M = 0$. At the interfaces, the gap function $\Delta(z)$ changes sign. Equation (14) is for the interfaces in superfluid ${}^3\text{He-B}$. At

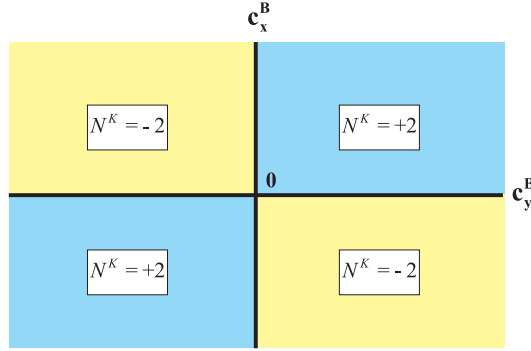


Fig. 6 Phase diagram of ${}^3\text{He-B}$ states at fixed $c_z^B > 0$, $\mu > 0$ and $m > 0$. At the phase boundaries the vacuum is gapless and corresponds to the 3+1 planar phase. The interface between the gapped states with different winding number N^K contains Majorana fermions.

the interface, one or two or all three components of speed c^B change sign. The latter case corresponds to the interface between two massive Dirac vacua in Eq. (15), where the mass parameter $M(z)$ changes sign across the interface.

If the interface separates bulk states with different values of topological invariants N^K , such interface contains the fermion zero modes – gapless branches of spectrum $E(p_x, p_y)$. There is an index theorem which relates the number of fermion zero modes to the difference of topological invariants of bulk states on two sides of the interface (see Refs.^{21,24} and references therein). In ${}^3\text{He-B}$, the topological charge changes sign if one of the speeds c^B (see Fig. 6) or all three speeds change sign. The latter case when all three speeds change sign across the interface is equivalent to the relativistic Ansatz in Eq.(12). That is why the spectrum of fermion zero modes at such wall can be obtained from applying the results of Ref.¹² to ${}^3\text{He-B}$. In the ${}^3\text{He-B}$ limit $mc_B^2 \ll \mu$, one obtains the spectrum of fermion zero modes at small momentum: $E^2 = v^2(p_x^2 + p_y^2)$ with velocity $v^2 \sim c_B^2 (mc_B^2/\mu)$. This velocity is much smaller than the velocity $v \sim c_B$ of fermions localized at the interface at which only one of the three speeds, c_z^B in Eq.(14), changes sign²⁵. The latter interface mimics the boundary of ${}^3\text{He-B}$ with specular reflection; the fermion zero modes at the boundary were discussed in Ref.²⁶.

5 Fermion zero modes on vortices

The simplified Hamiltonians describing the fermionic states in the core of a vortex with winding number n are correspondingly:

$$\hat{H} = \tau_3 (c\alpha \cdot \hat{\mathbf{p}} + \beta M - \mu_R) + \gamma_5 \Delta(r) (\tau_1 \cos n\phi + \tau_2 \sin n\phi), \quad (16)$$

$$\hat{H} = \tau_3 (c\alpha \cdot \hat{\mathbf{p}} - \mu_R) + \Delta(r) (\tau_1 \cos n\phi + \tau_2 \sin n\phi), \quad (17)$$

$$\hat{H} = \tau_3 \left(\frac{\hat{\mathbf{p}}^2}{2m} - \mu \right) + \frac{1}{2} \tau_1 \sigma \cdot \{c^B(r) \cos n\phi, \hat{\mathbf{p}}\} + \frac{1}{2} \tau_2 \sigma \cdot \{c^B(r) \sin n\phi, \hat{\mathbf{p}}\}, \quad (18)$$

$$\hat{H} = c\tau_3 \sigma \cdot \hat{\mathbf{p}} + M(r) (\tau_1 \cos n\phi + \tau_2 \sin n\phi). \quad (19)$$

Eq.(18) is the simplified Hamiltonian describing the most symmetric vortex in $^3\text{He-B}$: even the simplest vortex – most symmetric vortex with $n = 1$, which is called the o -vortex, – contains 5 components of the order parameter in the core²⁷.

Non-zero topological invariant describing the bulk superfluid gives rise to the gapless fermions living in the vortex core – fermion zero modes. As distinct from the bound states at the interfaces, the general index theorem which relates the existence of the fermion zero modes to the topological charge of the bulk state and the vortex winding number is still missing. The existing index theorems are applicable only to particular cases. In relativistic systems the index theorem relates the existence of the gapless fermions to the vortex winding number. There are also index theorems for fermions on vortices in non-relativistic systems: for the true fermion zero modes²⁸ and for the Caroli-de Gennes-Matricon²⁹ spectrum which has a small gap (the so-called minigap)³⁰. For the general case, which takes into account both the momentum-space topology of bulk state and the real-space topology of the vortex or other topological defects, the combined topology of the Green's function in the coordinate-momentum space $(\omega, \mathbf{p}, \mathbf{r})$ ^{31,28,21,32,33} must be used. Here we consider examples, which demonstrate that the connection between the topological charge N^K and the fermion zero modes on vortices. Other examples can be found in^{33,34}.

For $^3\text{He-B}$, which lives in the range of parameters where $N^K \neq 0$, the gapless fermions in the core have been found in Ref.¹⁸. On the other hand, in the BEC limit, when μ is negative and the Bose condensate of molecules takes place, there are no gapless fermions. Thus in the BCS-BEC crossover region the spectrum of fermions localized on vortices must be reconstructed. The topological reconstruction of the fermionic spectrum in the vortex core cannot occur adiabatically. It should occur only during the topological quantum phase transition in bulk, when the bulk gapless state is crossed. Such topological transition occurs at $\mu = 0$, see Fig. 4. At $\mu < 0$ the topological charge N^K nullifies and simultaneously the gap in the spectrum of core fermions arises, see Fig. 7. This is similar to the situation discussed in Ref.³⁵ for the other type of p -wave vortices, and in Refs. for Majorana fermions in semiconductor quantum wires^{36,37}.

This demonstrates that the existence of fermion zero modes is closely related to the topological properties of the vacuum state. The reconstruction of the spectrum of fermion zero modes at the topological quantum phase transition in bulk can be also seen for vortices in relativistic superconductors¹². Let us first consider the triplet superconductor, which incorporates the $^3\text{He-B}$ in the non-relativistic limit. The bulk states outside the circle $\mu_R^2 + \Delta^2 = M^2$ in Fig. 3 have $N^K \neq 0$, and vortices in such bulk states do have fermion zero modes¹², while the states inside the circle are topologically trivial, and they have no zero modes in the vortex core¹².

For singlet relativistic superconductor, the topological invariant N^K with $K = \tau_2$ is always zero, and thus does not support the gapless fermions in the core. However, at $M = 0$, i.e. for chiral fermions there is another topological charge N^K with $K = \tau_2\gamma_5$. This invariant is nonzero, see Fig. 5, and this is consistent with the existence of the fermion zero modes on vortices found by Nishida¹² for these superconductors at $M = 0$. The fermion modes become gapped, when $M \neq 0$ and the topological invariant N^K with $K = \tau_2\gamma_5$ ceases to exist.

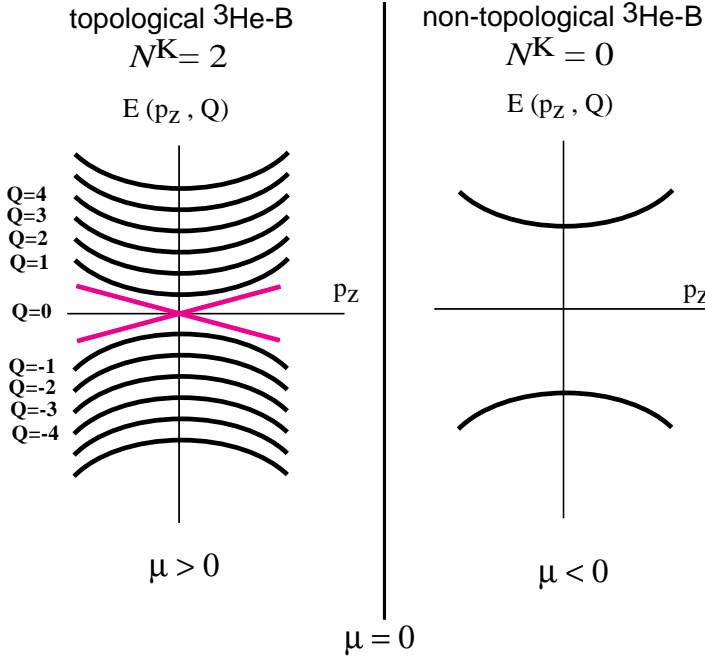


Fig. 7 Schematic illustration of spectrum of the fermionic bound states in the core of the most symmetric vortex with $n = 1$, the so-called o -vortex²⁷, in fully gapped spin triplet superfluid/superconductor of ${}^3\text{He-B}$ type. Q is the azimuthal quantum number – the generalized angular momentum of fermions in the vortex core. (*left*): Spectrum of bound state in the ${}^3\text{He-B}$, vortex which corresponds to the weak coupling limit with non-zero topological charge $N^K = 2$ ¹⁸. There are two fermion zero modes, which cross zero energy in the opposite directions. (*right*): The same vortex but in the topologically trivial state of the liquid, $N^K = 0$, does not have fermion zero modes. The spectrum of bound states is fully gapped. Fermion zero modes disappear at the topological quantum phase transition, which occurs in bulk liquid at $\mu = 0$. Similar situation may take place for strings in color superconductors in quark matter¹².

The generic example is provided by the fermions on relativistic vortices in Dirac vacuum in Eq. (19) discussed in Ref.¹⁵. The Dirac vacuum has the nonzero topological invariant, $N^K = \pm 1$, see Fig. 4. This is consistent with the existence of the fermion zero modes on vortices, found in Ref.¹⁵. The index theorem for fermion zero modes on these vortices can be derived using the topology in combined coordinate and momentum space. Extending the results of Ref.²⁸ for the spectral asymmetry index expressed via the Green's function, one obtains that the algebraic number of zero modes – branches which cross zero as function of p_z – is given by the 5-form constructed from the Green's function:

$$N_{\text{zm}} = N_5(p_z \rightarrow +\infty) - N_5(p_z \rightarrow -\infty), \quad (20)$$

$$N_5(p_z) =$$

$$\frac{1}{4\pi^3 i} \text{tr} \left[\int d^2 p d^2 x d\omega G \partial_{p_x} G^{-1} G \partial_{p_y} G^{-1} G \partial_x G^{-1} G \partial_y G^{-1} G \partial_\omega G^{-1} \right]. \quad (21)$$

In the simplest non-interacting case the Green's function is $G^{-1}(\omega, \mathbf{p}, x, y) = i\omega - H(\mathbf{p}, x, y)$. The 5-form invariant in terms of Green's function has been discussed also in^{21,38}. The Green's function for Hamiltonians (16)-(18) has singularity at $x = y = \mathbf{p} = \omega = 0$, and the integrals in (21) are over two 5D planes, $p_z = \text{const} > 0$ and $p_z = \text{const} < 0$, on two sides of the singularity.

Choosing another 5D surface around the Green's function singularity, the Eq.(20) can be rewritten in the following form:

$$N_{zm} = N_5, \quad (22)$$

$$N_5 = \frac{1}{4\pi^3 i} \text{tr} \left[\int d^3 p d\omega d\phi G \partial_{p_x} G^{-1} G \partial_{p_y} G^{-1} G \partial_{p_z} G^{-1} G \partial_{\omega} G^{-1} G \partial_{\phi} G^{-1} \right]. \quad (23)$$

The integral is now around the vortex line; the Green's function depends on $(\omega, \mathbf{p}, r, \phi)$ with fixed distance $r > 0$ from the vortex axis; and the azimuthal angle ϕ changes from 0 to 2π .

For the Dirac Hamiltonian (19), equation (23) gives $N_5 = n$, which reproduces the index theorem discussed in Ref.¹⁵: the algebraic number of fermion zero modes N_{zm} equals the vortex winding number n . The integration over the hyper-planes $p_z = \text{const}$ in Eq. (20) yields the number which approaches n in the asymptotic limit $|p_z| \gg |M|$.

However, the Dirac vacuum is marginal, since its Hamiltonian is non-compact^{21,9}. The ³He-B provides the regularization of the Dirac vacuum at large momentum \mathbf{p} ¹⁶, so that the modified Dirac Hamiltonian becomes compact. The modified Dirac vacuum with $1/m \neq 0$ in Fig. 4 is either trivial ($N^K = 0$) or topological ($N^K = \pm 2$). Correspondingly the fermion zero modes on a vortex either disappear or are doubled, Fig. 7.

The invariant N_5 does not give information on the fermion zero modes for Hamiltonians (16)-(18). For these Hamiltonians one obtains $N_5 = 0$, which is consistent with Fig. 7: two branches have opposite signs of velocity v_z and thus produce zero value for the algebraic sum of zero modes, $N_{zm} = 0$. To resolve the fermion zero modes in the systems where the branches cancel each other due to symmetry, the index theorem for the zero modes must be complemented by symmetry consideration.

6 Conclusion

We discussed here the fermion zero modes on vortices and interfaces which are protected by the topological invariant N^K . In all the systems, which we considered, the nonzero value of topological invariant in the bulk is associated with the existence of gapless fermions in the core of quantized vortices. The number of the fermion zero modes changes when the topological quantum phase transition occurs at which the bulk charge N^K changes. This suggests that there must be the generalized index theorem which relates the number of fermion zero modes on the vortex with the topology in the combined coordinate and momentum (\mathbf{p}, \mathbf{r}) space. An example is provided by Eqs. (20) and (22).

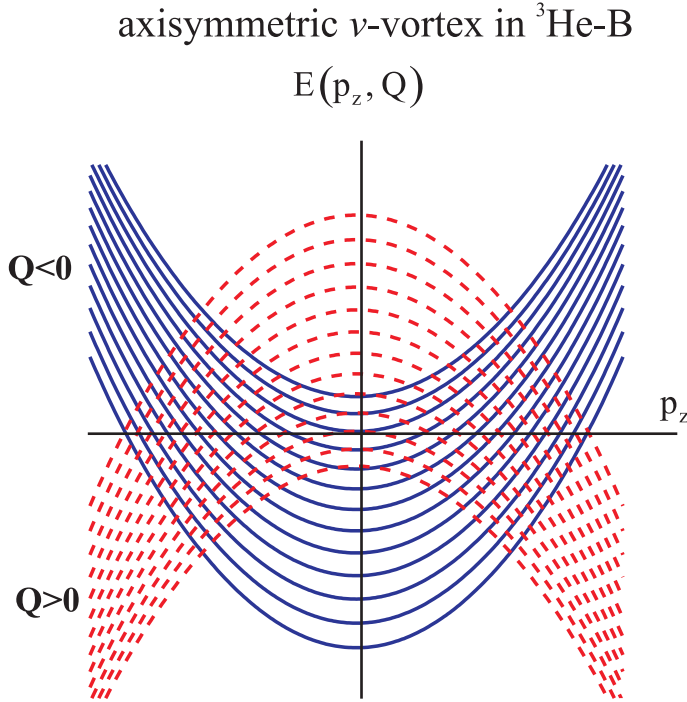


Fig. 8 Schematic illustration of spectrum of the fermionic bound states in the core of the real axisymmetric vortex in ${}^3\text{He-B}$ (the ν -vortex)³⁹. The fermion zero modes there belong to the class of one-dimensional Fermi surfaces. Existence of these zero modes is supported by the 3-form topological invariant in terms of the Green's function in combined (\mathbf{p}, \mathbf{r}) -space, $N_3 \propto \text{tr} \int (G \partial G^{-1})^3$, which gives rise to about $(\mu/mc_B^2)^{1/2} \sim 1000$ branches crossing zero energy²⁸.

We considered the most symmetric vortices. But in real superfluid ${}^3\text{He-B}$, the vortex cores have spontaneously broken symmetry: the broken parity or the broken parity combined with broken axial symmetry²⁷. The broken parity leads to many branches of gapless fermions forming the 1D Fermi liquids, as follows from the corresponding index theorem²⁸. Fig. 8 illustrates these branches in one of the vortices observed in ${}^3\text{He-B}$ – in the axisymmetric ν -vortex with the spontaneously broken parity in the core³⁹. Each Fermi surface (the point where the branch $E_n(p_z)$ crosses zero), belongs to the class of nodes of co-dimension 1 in Horava classification of topologically protected nodes⁴⁰. These are the most stable objects in momentum space, they are protected by the topological invariant²¹

$$N_1 = \text{tr} \oint_C \frac{dl}{2\pi i} G(p_0, \mathbf{p}) \partial_l G^{-1}(p_0, \mathbf{p}). \quad (24)$$

In general, the integral is taken over an arbitrary contour C around the Green's function singularity in the $D + 1$ momentum-frequency space $(i\omega, \mathbf{p})$; with $D = 1$ for our case of one-dimensional Fermi liquids in the vortex core. Due to nontrivial topological invariant, the Fermi surface survives the perturbative interaction and

exists even in case when quasiparticles are ill defined: in marginal, Luttinger and other exotic Fermi liquids⁴¹.

The topologically stable Fermi surface of co-dimension 1 may arise also on the surface of topological insulators forming the 2+1 Fermi liquids⁴². In ³He-B, these topologically stable lines of nodes may arise at the interface at which two of three speeds c^B change sign across the interface. The bulk states on two sides of the interface have the same topological invariant, see Fig. 6, nevertheless the density of states of the fermion zero modes at such interface is non-zero at $E = 0$ ²⁵, which is the signature of 1D Fermi surface.

We discussed here the fermion zero modes on straight vortices, which appear in the rotating vessel in superfluids or in applied magnetic field in superconductors. However, for quantum turbulence phenomena⁴³, the dynamics of fermion zero modes within the entangled and curved vortices could become important, providing the possible source of dissipation of turbulence at very low temperature. Topology of the fermion zero modes on curved and entangled vortices has been discussed in Ref.⁷.

Acknowledgements It is a pleasure to thank Yuriy Makhlin for discussions. This work is supported in part by the Academy of Finland, Centers of excellence program 2006-2011 and the Khalatnikov–Starobinsky leading scientific school (Grant No. 4899.2008.2). One of the authors (M.A.S.) was supported by “Dynasty” foundation.

References

1. M.Z. Hasan and C.L. Kane, Topological Insulators, arXiv:1002.3895.
2. B.A. Volkov, A.A. Gorbatsevich, Yu.V. Kopaev and V.V. Tugushev, Macroscopic current states in crystals, JETP **54**, 391–397 (1981).
3. B.A. Volkov and O.A. Pankratov, Two-dimensional massless electrons in an inverted contact, JETP Lett. **42**, 178–181 (1985).
4. Haijun Zhang, Chao-Xing Liu, Xiao-Liang Qi, Xi Dai, Zhong Fang and Shou-Cheng Zhang, Topological insulators in Bi_2Se_3 , Bi_2Te_3 and Sb_2Te_3 with a single Dirac cone on the surface, Nature Physics **5**, 438–442 (2009).
5. D. D. Osheroff, R. C. Richardson, and D. M. Lee, Evidence for a new phase of solid He-3, Phys. Rev. Lett. **28**, 885–888 (1972).
6. M.M. Salomaa and G.E. Volovik, Cosmiclike domain walls in superfluid $^3\text{He-B}$: Instantons and diabolical points in (\mathbf{k}, \mathbf{r}) space, Phys. Rev. **B 37**, 9298–9311 (1988).
7. Xiao-Liang Qi, T.L. Hughes, S. Raghu, and Shou-Cheng Zhang, Time-reversal-invariant topological superconductors and superfluids in two and three dimensions, Phys. Rev. Lett. **102**, 187001 (2009).
8. A. Kitaev, Periodic table for topological insulators and superconductors, AIP Conference Proceedings, Volume **1134**, pp. 22–30 (2009); arXiv:0901.2686.
9. A.P. Schnyder, S. Ryu, A. Furusaki and A.W.W. Ludwig, Classification of topological insulators and superconductors in three spatial dimensions, Phys. Rev. **B 78**, 195125 (2008).
10. M. Stone, Ching-Kai Chiu and A. Roy, Symmetries, Dimensions, and Topological Insulators: the mechanism behind the face of the Bott clock, arXiv:1005.3213.
11. R. Jackiw and C. Rebbi, Solitons with fermion number 1/2, Phys. Rev. **D 13**, 3398–3409 (1976).
12. Y. Nishida, Is a color superconductor topological? *Phys. Rev. D* **81**, 074004 (2010).
13. T. Ohsaku, BCS and generalized BCS superconductivity in relativistic quantum field theory: Formulation. Phys. Rev. **B 65**, 024512 (2001).
14. G.E. Volovik, Quantum phase transitions from topology in momentum space, in: "Quantum Analogues: From Phase Transitions to Black Holes and Cosmology", eds. W.G. Unruh and R. Schützhold, Springer Lecture Notes in Physics **718** (2007), pp. 31–73; cond-mat/0601372.
15. R. Jackiw and P. Rossi, Zero modes of the vortex-fermion system, Nucl. Phys. **B 190**, 681–691 (1981).
16. G.E. Volovik, Topological invariants for Standard Model: from semi-metal to topological insulator, JETP Lett. **91**, 55–61 (2010); arXiv:0912.0502.
17. Y. Nishida, L. Santos and C. Chamon, Topological superconductors as nonrelativistic limits of Jackiw-Rossi and Jackiw-Rebbi models, arXiv:1007.2201.
18. T. Sh. Misirpashaev and G.E. Volovik, Fermion zero modes in symmetric vortices in superfluid ^3He , *Physica B*, **210**, 338–346 (1995).
19. G.E. Volovik, Topological invariant for superfluid $^3\text{He-B}$ and quantum phase transitions, JETP Lett. **90**, 587–591 (2009).
20. S.M.A. Rombouts, J. Dukelsky and G. Ortiz, Quantum phase diagram of the integrable $p_x + ip_y$ fermionic superfluid, arXiv:1008.3406.

-
21. G.E. Volovik, *The Universe in a Helium Droplet*, Clarendon Press, Oxford (2003).
 22. G.E. Volovik, *The Superfluid Universe*, arXiv:1004.0597.
 23. V. Gurarie and L. Radzihovsky, Resonantly-paired fermionic superfluids, *Ann. Phys.* **322**, 2–119 (2007).
 24. B. Beri, Topologically stable gapless phases of time-reversal invariant superconductors, *Phys. Rev. B* **81**, 134515 (2010).
 25. G.E. Volovik, Fermion zero modes at the boundary of superfluid $^3\text{He-B}$, *JETP Lett.* **90**, 398–401 (2009); arXiv:0907.5389.
 26. Suk Bum Chung, Shou-Cheng Zhang, Detecting the Majorana fermion surface state of $^3\text{He-B}$ through spin relaxation, *Phys. Rev. Lett.* **103**, 235301 (2009); arXiv:0907.4394.
 27. M.M. Salomaa and G.E. Volovik, Quantized vortices in superfluid ^3He , *Rev. Mod. Phys.* **59**, 533–613 (1987).
 28. G.E. Volovik, Localized fermions on quantized vortices in superfluid $^3\text{He-B}$, *J. Phys.: Condens. Matter* **3**, 357–368 (1991).
 29. C. Caroli, P. G. de Gennes and J. Matricon, *Phys. Lett.* **9**, 307 (1964).
 30. G.E. Volovik, Vortex motion in fermi superfluids and Callan-Harvey effect, *JETP Lett.* **57**, 244–248 (1993).
 31. P.G. Grinevich and G.E. Volovik, Topology of gap nodes in superfluid ^3He : π_4 homotopy group for $^3\text{He} - B$ disclination, *J. Low Temp. Phys.* **72**, 371–380 (1988).
 32. J.C.Y. Teo and C.L. Kane, Majorana fermions and non-Abelian statistics in three dimensions, *Phys. Rev. Lett.* **104**, 046401 (2010).
 33. J.C.Y. Teo and C.L. Kane, Topological defects and gapless modes in insulators and superconductors, arXiv:1006.0690.
 34. Chi-Ken Lu and I.F. Herbut, Pairing symmetry and vortex zero-mode for superconducting Dirac fermions, arXiv:1007.3751.
 35. T. Mizushima and K. Machida, Vortex structures and zero-energy states in the BCS-to-BEC evolution of p -wave resonant Fermi gases, *Phys. Rev. A* **81**, 053605 (2010).
 36. R.M. Lutchyn, J.D. Sau and S. Das Sarma, Majorana fermions and a topological phase transition in semiconductor-superconductor heterostructures, *Phys. Rev. Lett.* **105**, 077001 (2010).
 37. Y. Oreg, G. Refael and F. von Oppen, Helical liquids and Majorana bound states in quantum wires, arXiv:1003.1145.
 38. Zhong Wang, Xiao-Liang Qi, Shou-Cheng Zhang, General theory of interacting topological insulators, arXiv:1004.4229.
 39. M. A. Silaev, Spectrum of bound fermion states on vortices in $^3\text{He-B}$, *Pis'ma ZhETF* **90**, 433-439 (2009).
 40. P. Hořava, Stability of Fermi surfaces and K -theory, *Phys. Rev. Lett.* **95**, 016405 (2005).
 41. T. Faulkner, N. Iqbal, Hong Liu, J. McGreevy, D. Vegh, From black holes to strange metals, arXiv:1003.1728.
 42. Liang Fu, Hexagonal warping effects in the surface states of topological insulator Bi_2Te_3 , *Phys. Rev. Lett.* **103**, 266801 (2009).
 43. V.B. Eltsov, R. de Graaf, R. Hanninen, M. Krusius, R.E. Solntsev, V.S. L'vov, A.I. Golov, P.M. Walmsley, Turbulent dynamics in rotating helium super-

fluids, Progress in Low Temperature Physics, Vol. XVI, p. 45–146 (2009),
arXiv:0803.3225.